Journal of Materials Chemistry B

Accepted Manuscript

ROYAL SOCIETY OF CHEMISTRY

www.rsc.org/materialsB

Table of Contents Entry

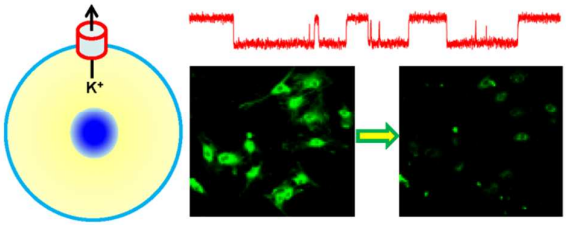

A synthetic K^+-like channel mediates K^+ outward flow to regulate vascular smooth muscle cell membrane potential, blood vessel tone and blood pressure.

A synthetic transmembrane segment derived from TRPV4 channel self-assembles into potassium-like channels to regulate vascular smooth muscle cell membrane potential

Zhiqiang Yu[b], Jie Li[a], Jinhang Zhu[a], Min Zhu[c], Feifei Jiang[a], Jin Zhang[a], Zhongwen Li[a], Mingkui Zhong[a], Justin Boy Kaye[b], Juan Du[a,*], Bing Shen[a,*]

[a]Department of Physiology, Anhui Medical University, Hefei, Anhui 230032, China.
[b]Center for BioEnergetics, The Biodesign Institute, and Department of Chemistry and Biochemistry, Arizona State University, Tempe, AZ 85287, USA.
[c]Hefei Institutes of Science, Chinese Academy of Sciences, Hefei, Anhui 230032, China.

*Address correspondence to Bing Shen, Ph.D., Juan Du, Ph.D.
Department of Physiology
Anhui Medical University
81 Meishan Road, Hefei, Anhui 230032, China
Fax: +86-0551-65161126, Tel: +86-0551-65161132
Email: shenbing@ahmu.edu.cn, dujuan@ahmu.edu.cn

Abstract:

Synthetic ion channels represent a new approach to mimicking natural ion channels and developing therapeutic drugs to restore ion channel dysfunction. The large superfamily of transient receptor potential (TRP) channels involved in numerous biological processes is an important and potent therapeutic target for various human diseases. In the present study, a synthetic peptide whose sequence is from the fourth transmembrane segment of TRPV4 is found that it is capable of self-assembling into potassium (K^+)-like ion channels designated as TRP-PK1 in the membranes of liposomes and live cells. TRP-PK1 effectively mediates K^+ flow across the cell membrane to regulate the membrane potential. TRP-PK1 is also able to relax agonist-induced vessel contraction and regulate the resting blood pressure by hyperpolarizing the vascular smooth muscle cell membrane potential. TRP-PK1 represents a novel lead compound for mimicking K^+ channels and treating hypertension, heart rate disorder, as well as other K^+ channel dysfunction-induced diseases. The present study also sheds new light into the mimic ion channel function and the significant utilization of natural biological sources.

Key words: Synthetic ion channels; K^+ channel; Vascular smooth muscle cell; Membrane potential; Hypertension.

1. Introduction

The transient receptor potential (TRP) superfamily is a group of cation channels. All TRPs are formed by four subunits, and every subunit includes six transmembrane domains (S1-S6).[1-3] The loop between S5 and S6 makes up the pore region of the TRP channel.[1] The majority of TRP channels displays a Ca^{2+} ion-permeable feature, thus, they usually mediate Ca^{2+} signaling and exert numerous physiologic functions in variety of tissues.[4-8] The dysfunction of TRP channel has been linked with diverse human diseases, such as autosomal dominant polycystic kidney disease caused by mutations in the *PKD2* or *PKD1* gene and autosomal dominant metatropic dysplasia caused by mutations in the *TRPV4* gene.[9-13] In recent years, scientists specializing in a broad range of study areas have made rapid progress in this field.

Synthetic ion channels represent a novel strategy for ion channel drug development.[14-17] However, it remains a great challenge to rationally design an artificial ion channel from scratch, with the ion selectivity as precise as that of its natural counterpart. As an alternative approach, a "strip-down" version of the ion channel may be worth the attention, which simplifies sample synthesis, as well as largely retains the activity. Several studies have shown that a peptide segment of the transmembrane domain of ion channel proteins is capable of self-assembling into ion channels in artificial or cell membranes.[14, 15, 18-21] These peptide-based channels can at least partially mimic natural ion channel functions.[14, 15, 18, 19, 21] However, little functional properties in the biological system were characterized in these studies. Therefore, the lack of biological characteristics in these studies obstructs our enthusiasm to dig out their potential application in future. Here, we not only proved that a synthesized peptide derived from TRPV4 protein can form an ion channel to transport K^+ ions, but also used a set of biological experiments to the characterize its functional role and potential application in cardiovascular system.

In the present study, we determined that a peptide segment (AYLAVMVFALVLGWMNALYFTRGL) from the fourth transmembrane domain of TRPV4, designated as TRP-PK1, could incorporate into both liposomes and live cell membranes to transport K^+ ions. Thus the synthesized peptide may presumably form a K^+-like channel by self-assembly and be a novel lead compound for mimicking K^+ channels.

2. Experimental

2.1. Materials

Wang resin, Fmoc-amino acids and coupling reagents for peptide synthesis were purchased from GL biochem (Shanghai, China). PBFI and $DiBAC_4(3)$ fluorescence dyes were purchased from Invitrogen. POPC (1-palmitoyl-2-oleoyl-s*n*-glycero-3-phosphocholine) and PS (L-α-phosphatidylserine) were purchased from Avanti Polar Lipids Inc. Safranin O, 4-aminopyridine and phenylephrine were obtained from Sigma.

2.2. Solid phase peptide synthesis of TRP-PK1

TRP-PK1 peptide was synthesized manually according to standard protocols using the Fmoc/tert-butyl strategy. The first C-terminal Leu residue was preloaded on amino acid–Wang polystyrene resin on a 0.2 mmol scale. The coupling reaction was carried out using 5 equivalents (relative to resin loading) of amino acid: HBTU: DIEA (1:1:2) for 2 h. The N-terminal Fmoc deprotection was achieved using 20% piperidine in DMF for 2 x 10 min. After complete peptide chain assembly and removal of the N-terminal Fmoc group, cleavage from resin was achieved using 1 mL of cocktail reagent per 0.025 mmol of crude peptide (cocktail reagent: 90% TFA, 5% TIS, and 5% water) for 3 h at room temperature. The peptide mixture was precipitated and washed twice with cold ether and lyophilized at −20 °C.

2.3. Purification and identification

According to the previous report with minor modification, the resulting crude peptides were purified by reversed-phase HPLC using a Vydac C18 column (10 mm × 250 mm) eluted with a linear gradient of acetonitrile in 0.1% TFA in water, changing from 55 to 85% solution B (0.1% TFA in acetonitrile) in solution A (0.1% TFA in water) for 25min at a 3 ml/min flow rate.[22] Chromatograms were monitored at 220 nm. Identification of synthetic peptide was confirmed by ESI mass spectrometer (Bruker Daltonics, Bellerica, MA, U.S.A.).

2.4. Animals and VSMC culture

All animal experiments were conducted in accordance with the regulation of the U.S. National Institute of Health (NIH publication No.8523) and approved by the Institutional Animals Care and Use Committee of Anhui Medical University. 4-6 week old male C57 mice were killed by overdose of CO_2. The thoracic aorta was quickly dissected free and placed in Krebs Henseleit solution containing (in mM): NaCl 118, KCl 4.7, $CaCl_2$ 2.5, KH_2PO_4 1.2, $MgSO_4$ ($7H_2O$) 1.2, $NaHCO_3$ 25.2 and glucose 11.1. Under a dissecting microscope, adhering perivascular tissue was carefully removed.

Next the vessel was opened longitudinally and the endothelium layer was scraped. The vessel segment was cut into 2×2 mm blocks. The tissue blocks were placed on the bottom of 3×3 cm dish. After the tissue blocks were cultured in an incubator at 37 ^{o}C for several minutes, the culture medium DMEM supplemented with 10% FBS, 100 μg/ml penicillin, and 100 U/ml streptomycin was carefully added. The vascular smooth muscle cells grew out from the tissue blocks after 4-7 days.

2.5. Electrophysiology

Single-channel recording was performed on giant liposomes according to our previous studies.[16] Briefly, POPC (80 mg, 105 μM) and PS (20 mg, 25 μM) with an 80:20 (w/w) ratio were dissolved in 2 mL of distilled water. The mixture was intermittently stirred, vortexed for 20 min, and then sonicated for 10 min under nitrogen protection. The suspension was centrifuged at 160,000 g for 1 h, and the pellet was resuspended with 200 μL of 10 mM MOPS buffer (pH 7.2) containing 5% (w/v) ethylene glycol. The resuspended sample was deposited on a clean glass slide in a 15 μL aliquot and submitted to partial dehydration (3–6 h) at 4°C. Before use, the sample was rehydrated for 10 h at 4°C by using 15 μL of 200 mM KCl, NaCl or NMDG-Cl. For patch-clamp measurements of giant liposomes, 1–3 μL of hydrated liposome suspension was dropped on a Petri dish and diluted with bath solutions. Single-channel currents through giant liposome membranes in presence of TRP-PK1 were measured with cell-attached configuration of the patch-clamp technique. Patch pipettes (resistance, 7–10 MΩ) were filled with internal pipette solution containing (in mM): 200 KCl (or NMDG-Cl), 10 HEPES, pH 7.4. The bath solution was composed of (in mM) 200 KCl (or NMDG-Cl), 10 HEPES, pH 7.4. Single channel currents were recorded with EPC 10 patch clamp amplifier (HEKA Elektronik, Lambrecht/Pfalz, Germany) in voltage-clamp mode. The data was recorded and analyzed by Pulse/PulseFit 8.7 software (HEKA). Pipette and membrane capacitance were electronically compensated. Single channel currents were digitized at 0.15 ms sampling interval, filtered at 0.5 kHz.

2.6. Intravesicular K^+ detection via PBFI dye

POPC and PS with an 80:20 (w/w) ratio were dissolved in a $CHCl_3$/MeOH mixture. The solvent was evaporated under reduced pressure and the thin film was dried. The lipid film was hydrated in 1.3 mL of intravesicular solution containing 500 μM PBFI, 100 mM NMDG-Cl, 10 mM HEPES (pH 6.8) for NMDG-Cl-filled liposomes or 100 mM KCl, 10 mM HEPES (pH 6.8) for KCl-filled liposomes for 2h. 5 freeze-thaw cycles from liquid nitrogen to water at RT were applied during hydration. Eventually,

the liposomes were made via 25 extrusions through a 100 nm polycarbonate membrane that afforded a suspension of large unilamellar vesicles with an average diameter of 100 nm. The PBFI was excited at 340- 345 nm and at 370-390 nm while fluorescent signal was measured at 450-550 nm to determine the intravesicular K^+ concentration. Changes in intravesicular K^+ concentration were displayed as the ratio of fluorescence relative to the intensity before the application of extracellular TRP-PK1 (Ft/F0).

Whole-cell current was recoded as our previous report.[23] HEK293 cells were placed in NPSS and the pipette was filled with solution containing (in mM) 140 KCl, 1 $MgCl_2$, 10 HEPES, 5 EGTA, 5 Na_2ATP (pH 7.2 with KOH). The cells were held at +60 mV and voltage steps ranging from –100 to +100 mV were applied for 200 ms in 20-mV step increments. The data was recorded and analyzed by Pulse/PulseFit 8.7 software (HEKA). In the ion permeability experiment, ramp recording from –100 to +100 mV for 200 ms was applied repeatedly with 3 sec intervals in HEK293 cells. The pipette solution contained 150 KCl, 10 HEPES, 5 EGTA (in mM, pH 7.2 with KOH). The bath solution was 150 KCl or NaCl or CsCl and 10 HEPES (in mM, pH 7.4 with their alkalis). The bath solutions with different ion compositions were perfused sequentially. The reverse potential was recorded and analyzed by the Pulse/PulseFit 8.7 software. The relative ion permeability ratio was calculated according to Nernst equation after the removal of the liquid junction.

2.7. Membrane potential measurement in liposomes

Similar to the above method, liposomes contained 100 mM KCl, 10 mM HEPES (pH 6.8) were prepared. Before the experiment, the liposomes were placed in NaCl-HEPES buffer (100 mM NaCl, 10 mM HEPES, 60 nM safranin O, pH 6.8). Safranin O was excited at 520 nm and the fluorescent signal was monitored at 580 nm. Changes in liposome membrane potential were displayed as the ratio of fluorescence relative to the intensity before the application of extracellular TRP-PK1 (Ft/F0).

2.8. Membrane potential measurement in the primary cultured VSMCs

Membrane potential was measured as described previously.[24] Briefly, primary cultured VSMCs were loaded with 100 nM $DiBAC_4$ (3) in a normal physiological saline solution (NPSS) that contained in mM: 140 NaCl, 5 KCl, 1 $CaCl_2$, 1 $MgCl_2$, 10 glucose, 5 HEPES, pH 7.4 at 37^{o}C for 10 min. $DiBAC_4$(3) is a membrane potential-sensitive dye, the fluorescence of which is enhanced when the dye enters the cell membrane as a result of membrane depolarization. Conversely, hyperpolarization

leads to efflux of the probe and a decrease in fluorescence intensity. The membrane potential of VSMC was depolarized by 60 mM high K^+ solution containing (in mM): 85 NaCl, 60 KCl, 1 $CaCl_2$, 1 $MgCl_2$, 10 glucose, 5 HEPES, pH 7.4. $DiBAC_4(3)$ was excited at 488 nm and the emission light was monitored at 516 nm via Leica SP5 confocal laser scanning system.

2.9. Vessel tension measurement

Vessel tension was measured as described previously.[25] Briefly, the vessel rings without endothelium were mounted onto two thin stainless steel holders, one of which was connected to a force displacement transducer and the other to a movable device that allowed the application of a passive tension of 550 – 600 mg. The mounted rings were placed in 2 mL organ baths containing the Krebs Henseleit solution, kept at 37 °C and continuously bubbled with a gas mixture of 95 % O_2 and 5 % CO_2 to maintain a pH of 7.4. The isometric tension was recorded and analyzed by a data acquisition and analysis system (BL-420E+, Chengdu technology & Market Corp. China).

2.10. Blood pressure measurement

4-6 week old male C57 mice were anaesthetized with pentobarbital sodium (100 mg/kg). The right common carotid artery was cannulated and blood pressure was continuously measured. The blood pressure was acutely elevated by intravenous infusion of 1 mg/25 g TRP-PK1 or solvent control (DMSO) through the mouse carotid vein. The blood volume of one mouse is about 1.5 ml (weight: 25 g). Given that the bioavailability of TRP-PK1 in the body is much lower than that in the vessel tension measurement, the dosage of TRP-PK1 in the animal experiment was ~10 times higher than the largest concentration used in the vessel tension measurement. Peak values of mean arterial pressure (MAP) in response to TRP-PK1 and DMSO were analyzed by Chart 5.0 software.

2.11. Statistical analysis

All experiments were repeated at least three times. In membrane potential measurement, *n* represents the independent experiment and the value of one experiment was the average of the data from 40-50 cells. Results were expressed as mean values ± standard error (mean ± SE). Significance differences between the treatments and the controls were determined based on Student's t test. A level of $P < 0.05$ was considered to be significant.

3. Results

3.1. Peptide synthesis and characterization

The crude peptide was purified by reversed-phase HPLC using a Vydac C18 column, RP-HPLC analysis of the crude cleavage product showed a single major peak with a purification of 90% with a retention time of 21.24 min (Fig. 1). The mass of the $[M+3H]^{3+}$ ions determined by ESI mass spectrometry were 907.95 Da for the purified TRP-PK1, in agreement with the calculated $M + H^+$ (2720.36) mass of synthetic peptide (Fig. 2).

3.2. Electrophysiological properties of TRP-PK1

First, patch clamp single channel recording, a very powerful tool in ion channel study [26], was used to characterize the TRP-PK1 ion channel in giant liposomes. The giant liposomes were prepared from 1-palmitoyl-2-oleoyl-*sn*-glycero-3-phosphocholine (POPC) and L-α-phosphatidylserine (PS) at a 4:1 ratio and blended with 500 nM TRP-PK1 before single-channel recording. The single-channel current was recorded in both extravesicular and intravesicular solutions containing 200 mM KCl. Fig. 3A shows a set of typical single-channel currents within the physiologic range of –40 mV to –100 mV. The conductance of the channel is 51.5 pS, as calculated using a current–voltage curve (Fig. 3C). However, when the solutions at both sides of the membrane were changed into 200 mM NMDG-Cl with the same TRP-PK1 application, no current could be elicited even when the membrane potential was depolarized to –180 mV (Fig. 3B). $NMDG^+$ is a large organic molecule that cannot penetrate ion channel pores. Therefore, the data strongly suggest that TRP-PK1 is capable of forming an ion channel permeable to cation ions in the liposome membrane. The TRP-PK1 channels also exhibited multiple conductances similar to other reported synthetic ion channels (data not shown).[18, 27-29] This phenomenon is probably caused by the resulting different pore sizes when ion channels randomly self-assemble in the membrane.[18, 27-29]

The plasma membrane of living cells contains numerous membrane proteins that make the membrane much more rigid than artificial liposome membranes. Determining whether the TRP-PK1 channels form a functional K^+-like channel in the cell membrane is of particular interest to us. Whole-cell recording was performed in HEK293 cells which were widely used in the ion channel study because HEK293 cells have low ion channel background. K^+ current was recorded from –100 to +100 mV step by step. Data show that 5 μM TRP-PK1 significantly enhanced K^+ current

and reverse potential shifted to the left (Fig. 4A-4C). In addition, we used voltage-gated K^+ channel inhibitor 4-aminopyridine (4-AP) to treat the cells. 100 μM 4-AP inhibited endogenous K^+ channel in HEK293 cells (Fig. 4B, 4C and 4D). Therefore K^+ current reduced, however, 4-AP did not notably inhibit TRP-PK1 channel current (Fig. 4D and 4E).

To identify the ion permeability of the TRP-PK1 channel, ramp patch clamp recording was employed (Fig. 4F). We utilized symmetric 150 mM K^+ between intracellular and extracellular sides of HEK293 cells. The reverse potential changes with or without 5 μM TRP-PK1 were determined when extracellular K^+ was replaced by equimolar Na^+ or Cs^+. The data indicate that when extracellular K^+ was exchanged into Na^+ or Cs^+ the reverse potential shifted to the left. Meanwhile, the outward current was increased accompanying with decreased inward current (Fig. 4G and 4H). After the subtraction of the effect of endogenous channels in the cells, the cation ion permeability ratio of the TRP-PK1 channel was resolved. The data show that the ion permeability ratio of K^+ : Cs^+ : Na^+ was 1 : 0.82 : 0.36 from 3-5 cells, i.e., the monovalent cation transport activity of the TRP-PK1 channel follows the sequence $K^+ > Cs^+ > Na^+$. Thus, the result strongly suggested that the TRP-PK1 channel is characteristics of a K^+ channel beyond a Na^+ channel.

3.3. K^+ permeability of TRP-PK1

To confirm further the K^+ permeability of the TRP-PK1 channel, the K^+-sensitive fluorescent dye PBFI was employed.[30] Liposomes containing 100 mM NMDG-Cl and 500 μM PBFI were prepared. Before the experiment, the liposomes were suspended in a 100 mM KCl solution. The PBFI fluorescence in the liposomes was measured with a spectrometer. The signal increment represented PBFI and K^+ ion binding. The results show that 5 μM TRP-PK1 application markedly increased the PBFI fluorescence intensity compared with the solvent control (DMSO) (Fig. 5). In the result, DMSO also induced a small increase of the fluorescent signal. It may be because DMSO affected the refraction of the extravesicular solution or ruptured some liposomes with poor quality, which increased basal fluorescent intensity. This finding indicates that TRP-PK1 mediates the flow of K^+ into the liposomes. Therefore, the data prove that the TRP-PK1 channel effectively mediates K^+ flow across a lipid membrane.

3.4. Membrane potential regulation of TRP-PK1

Liposomes filled with 100 mM KCl were prepared and re-suspended in a 100 mM NaCl solution containing 60 nM safranin O, a membrane potential-sensitive

fluorescence dye. The fluorescence signal was recorded and the increment of fluorescence density was deemed to represent hyperpolarization. The data indicate that 5 μM TRP-PK1 unambiguously hyperpolarizes the KCl-filled liposome membrane potential compared to the solvent control (Fig. 6).

Primary cultured VSMC was loaded with a membrane potential fluorescent dye $DiBAC_4(3)$. The fluorescence density decrease represents hyperpolarization. Remarkably, 0.1 and 1 μM TRP-PK1 strongly induced hyperpolarization in a dose-dependent manner (Fig. 7).

3.5. TRP-PK1 attenuated agonist-induced mice aorta contraction

Considering TRP-PK1 can decrease the membrane potential of VSMCs, theoretically, it could regulate vessel tension. To verify this hypothesis, vessel tension measurements were made to investigate the effects of TRP-PK1 on vessel contraction. Mouse aortic rings without an endothelial layer were constricted with the α receptor agonist phenylephrine (Phe; 10 μM). Phe acts on the α receptor located on the VSMC plasma membrane to induce increased $[Ca^{2+}]_i$ through several mechanisms, including membrane depolarization.[31] After the mouse aortic rings without endothelium were induced to contract with 10 μM Phe up to the plateau, 1 μM to 30 μM TRP-PK1 was accumulatively added to the bath solution. The data show that TRP-PK1 significantly relaxed the Phe-induced contraction dose dependently (Fig. 8A and 8B). This effect is completely different from a chloride channel-like compound, which strongly reduced high K^+ solution-induced contraction but not relaxed the Phe-induced contraction in our previous study.[24] This result confirms the capability of TRP-PK1 to regulate vessel tension by repolarizing and/or hyperpolarizing the VSMC membrane potential.

3.6. TRP-PK1 reduced mouse blood pressure

To evaluate the potential value of TRP-PK1 as an alternative clinical treatment for hypertension, the effect of TRP-PK1 on mouse blood pressure was investigated. Under anesthesia, the mouse mean arterial pressure (MAP) was continuously measured from the common carotid artery via a pressure transducer. 1 mg/25 g TRP-PK1 bolus injection through the mouse carotid vein significantly decreased the MAP compared to the solvent control (Fig. 9).

4. Discussion

In the present study, we synthesized a 24aa-peptide TRP-PK1, and recorded its single

channel and whole cell currents in the liposomes and HEK293 cells. TRP-PK1 transported K^+ ions to regulate the liposome and VSMCs membrane potential, and dose-dependently relaxed the mouse aorta. In addition, TRP-PK1 injection significantly decreased the mouse MAP.

A liposome has a zero background of ion flow; thus, it is a robust tool for studying the function of synthetic ion channels.[32] In the present study, the results from single channel recording and K^+ fluorescence implicate that TRP-PK1 may form a K^+ permeable channel in liposomes. In addition, the addition of TRP-PK1 to the solution strongly hyperpolarized the KCl-filled liposome membrane potential in a 100 mM NaCl solution. In this system, Cl^- has a symmetric distribution across the lipid membrane. Thus, the contribution of Cl^- to membrane potential hyperpolarization could be safely excluded. Given so, the hyperpolarization may be attributed to the efflux of K^+. Therefore, the data provide the evidence that the TRP-PK1 channel is capable of regulating membrane potential by mediating the K^+ flow across a lipid membrane.

The whole cell recording data indicate that the TRP-PK1 channel not only enhanced the K^+ current in HEK293 cells but also was not inhibited by the K^+ channel inhibitor 4-AP. The results suggest that TRP-PK1 can form a K^+ permeable channel in the live cell membrane. Indeed it is difficult to determine how the TRP-PK1 peptides form an ion channel and what the structure of the TRP-PK1 channel is in the cell membrane. Based on the original property in the TRPV4 channels, the TRP-PK1 peptide should be hydrophobic and form an α-helix in the cell membrane. We speculate that maybe several TRP-PK1 peptides clustered parallel together to self-assemble a K^+ permeable pore. Therefore, the TRP-PK1 channel structure and gating mechanism will be totally different from the native K^+ channel. This probably is the reason that the native K^+ channel inhibitor did not inhibit the TRP-PK1 channel. In the whole cell ramp recording, the cation ion permeability ratio of the TRP-PK1 channel was determined by comparing the reverse potential. The result indicates that the permeable ions of the TRP-PK1 channel greatly prefers K^+ ion to Na^+ ion. Thus, these results further demonstrate that the TRP-PK1 peptide enhances the cell membrane K^+ permeability.

The sequence of TRP-PK1 is obtained from the fourth transmembrane domain (S4) of TRPV4, but this does not mean that the TRP-PK1 channel was expected to have similar eletrophysiological property to TRPV4. Because the pore-forming sequence of the TRP-PK1 channel is completely different from that of TRPV4 channel. The

TRP-PK1 channel uses itself to form the channel pore, but TRPV4 utilizes the loop between S5 and S6. The amino acid sequences of the TRP-PK1 and TRPV4 loop between S5 and S6 (DQSNCTVPSYPACRDSETFSAFLLDLFKLTI) are notably different. Meanwhile, the channel filter determining the ion selectivity is located in the pore region exactly. Therefore, it should be different in the filter of the two channels as well as the ion selectivity. Taken together, TRPV4 and the TRP-PK1 channels are two different ion channels entirely.

Because our synthesis of the ion channel aims at the potential in the clinical applications, biocompatibility is of great importance by all means. In live cells, the crucial function of K^+ channels is to control the cell membrane potential.[33] The change in the cell membrane potential in response to endogenous or exogenous stimuli is a crucial factor that affects the activity of excitable cells such as muscular cells, neurons, and gland cells.[34] The contraction of VSMCs directly induces increased vessel tension and blood pressure because of the increased intracellular Ca^{2+} concentration ($[Ca^{2+}]_i$) caused by the opening of voltage-gated Ca^{2+} channels (VGCCs) located in the plasma membrane. Membrane potential depolarization activates VGCCs to mediate Ca^{2+} influx, which triggers excitation–contraction coupling, which eventually leads to VSMC contraction (Fig. 10). Otherwise, repolarization and hyperpolarization lead to VSMC relaxation.[35] The K^+ channel opening in the plasma membrane causes repolarization and hyperpolarization because of the high K^+ gradient between the intracellular and extracellular fluids. In the present cell-based study, 0.1 and 1 μM TRP-PK1 induced significant hyperpolarization in a dose-dependent manner. Moreover, TRP-PK1 dose-dependently reduced Phe-induced mouse aortic ring contraction. This result demonstrates that TRP-PK1 is able to incorporate into VSMC membranes, form the K^+ permeable channel, and regulate the membrane potential and blood vessel tension.

In several human diseases such as hypertension and diabetes, the $[Ca^{2+}]_i$ in the VSMCs of patients is relatively higher than in healthy individuals because the patient's body is in a high oxidative state. This condition routinely leads to increased vessel tension, an important factor in the development of hypertension. To restore the $[Ca^{2+}]_i$ in the VSMCs to normal, several approaches can be utilized, including the direct inhibition of the VGCCs via specific blockers, hyperpolarization of the VSMC membrane potential to suppress VGCC activity indirectly, and so on. Among these, a couple of VGCC inhibitors have been widely used in the clinical treatment of hypertension. However, the second point as an alternative treatment is still not well

developed. In the present study, we used the TRP-PK1 channel to suppress VGCCs activity of the VSMCs which cause the relaxation of the blood vessel. Therefore, we hypothesized that TRP-PK1 could decrease the blood pressure. The data show that TRP-PK1 bolus injection significantly decreased the MAP. This result provides good evidence of the potential of TRP-PK1 in future clinical applications for hypertension treatment. TRP-PK1 is also very promising for the treatment of other K^+ channel dysfunction-induced diseases, such as heart rate disorder, epilepsy, periodic paralysis, and so on.[36]

5. Conclusion

In the present study, we developed a synthetic K^+-like channel, TRP-PK1, which is capable of incorporating into both artificial and living cell membranes. TRP-PK1 effectively mediates K^+ flow across the plasma membrane to regulate the cell membrane potential. Through this mechanism, TRP-PK1 regulates the membrane potential of mouse VSMCs to suppress agonist-induced vessel contraction and decreases the circulating blood pressure. Therefore, TRP-PK1 is a new lead compound for mimicking K^+ channels and developing therapeutic drugs.

Acknowledgments

This work was supported by Grants from Natural Science Foundation of China (81371284, 30800384, 61273324), Scientific Research of BSKY from Anhui Medical University (XJ200913, XJ201106), Anhui Provincial Natural Science Foundation (11040606M171, 1108085J11), and Young Prominent Investigator Supporting Program from Anhui Medical University. We thank Dr. Li Xiang for very constructive and valuable advice to improve this study; Dr. Cun Shujian for kindly language polishing and suggestions.

Reference

1. R. Latorre, C. Zaelzer and S. Brauchi, *Q Rev Biophys*, 2009, **42**, 201-246.
2. Z. Pan, H. Yang and P. S. Reinach, *Hum Genomics*, 2011, **5**, 108-116.
3. L. J. Wu, T. B. Sweet and D. E. Clapham, *Pharmacol Rev*, 2010, **62**, 381-404.
4. B. Colsoul, R. Vennekens and B. Nilius, *Rev Physiol Biochem Pharmacol*, 2012, **161**, 87-110.
5. D. X. Zhang and D. D. Gutterman, *J Cardiovasc Pharmacol*, 2011, **57**, 133-139.
6. P. C. Yu and J. L. Du, *Cell Mol Life Sci*, 2011, **68**, 3815-3821.
7. S. Earley and J. E. Brayden, *Clin Sci (Lond)*, 2010, **119**, 19-36.

8. D. Dadon and B. Minke, *Int J Biochem Cell Biol*, 2010, **42**, 1430-1445.
9. B. Nilius and G. Owsianik, *Pflugers Arch*, 2010, **460**, 437-450.
10. P. Holzer, *Pharmacol Ther*, 2011, **131**, 142-170.
11. M. M. Moran, M. A. McAlexander, T. Biro and A. Szallasi, *Nat Rev Drug Discov*, 2011, **10**, 601-620.
12. D. Krakow, J. Vriens, N. Camacho, P. Luong, H. Deixler, T. L. Funari, C. A. Bacino, M. B. Irons, I. A. Holm, L. Sadler, E. B. Okenfuss, A. Janssens, T. Voets, D. L. Rimoin, R. S. Lachman, B. Nilius and D. H. Cohn, *Am J Hum Genet*, 2009, **84**, 307-315.
13. J. J. Grantham, S. Mulamalla and K. I. Swenson-Fields, *Nat Rev Nephrol*, 2011, **7**, 556-566.
14. W. Grosse, L. O. Essen and U. Koert, *Chembiochem*, 2011, **12**, 830-839.
15. U. Bukovnik, J. Gao, G. A. Cook, L. P. Shank, M. B. Seabra, B. D. Schultz, T. Iwamoto, J. Chen and J. M. Tomich, *Biochim Biophys Acta*, 2011.
16. X. Li, B. Shen, X. Q. Yao and D. Yang, *J Am Chem Soc*, 2007, **129**, 7264-7265.
17. B. A. McNally, W. M. Leevy and B. D. Smith, *Supramol Chem*, 2007, **19**, 29-37.
18. V. Nunukova, E. Urbankova, M. Jelokhani-Niaraki and R. Chaloupka, *Biopolymers*, 2010, **93**, 718-726.
19. M. Mustata, R. Capone, H. Jang, F. T. Arce, S. Ramachandran, R. Lal and R. Nussinov, *J Am Chem Soc*, 2009, **131**, 14938-14945.
20. R. Verma, C. Malik, S. Azmi, S. Srivastava, S. Ghosh and J. K. Ghosh, *J Biol Chem*, 2011, **286**, 24828-24841.
21. M. Oblatt-Montal, G. L. Reddy, T. Iwamoto, J. M. Tomich and M. Montal, *Proc Natl Acad Sci U S A*, 1994, **91**, 1495-1499.
22. Z. Yu, R. M. Schmaltz, T. C. Bozeman, R. Paul, M. J. Rishel, K. S. Tsosie and S. M. Hecht, *J Am Chem Soc*, 2013, **135**, 2883-2886.
23. B. Shen, X. Li, F. Wang, X. Yao and D. Yang, *PLoS One*, 2012, **7**, e34694.
24. X. Li, B. Shen, X. Q. Yao and D. Yang, *J Am Chem Soc*, 2009, **131**, 13676-13680.
25. B. Shen, C. L. Ye, K. H. Ye, L. Zhuang and J. H. Jiang, *Acta Pharmacol Sin*, 2009, **30**, 1488-1495.
26. O. P. Hamill, A. Marty, E. Neher, B. Sakmann and F. J. Sigworth, *Pflugers Arch*, 1981, **391**, 85-100.
27. P. Prangkio, D. K. Rao, K. D. Lance, M. Rubinshtein, J. Yang and M. Mayer, *Biochim Biophys Acta*, 2011, **1808**, 2877-2885.
28. A. Schrey, A. Vescovi, A. Knoll, C. Rickert and U. Koert, *Angew Chem Int Ed Engl*, 2000, **39**, 900-902.
29. A. V. Starostin, R. Butan, V. Borisenko, D. A. James, H. Wenschuh, M. S. Sansom and G. A. Woolley, *Biochemistry*, 1999, **38**, 6144-6150.
30. K. Meuwis, N. Boens, F. C. De Schryver, J. Gallay and M. Vincent, *Biophys J*, 1995, **68**,

2469-2473.

31. G. Bastin and S. P. Heximer, *Arch Biochem Biophys*, 2011, **510**, 182-189.
32. M. Bally, K. Bailey, K. Sugihara, D. Grieshaber, J. Voros and B. Stadler, *Small*, 2010, **6**, 2481-2497.
33. H. Wulff, N. A. Castle and L. A. Pardo, *Nat Rev Drug Discov*, 2009, **8**, 982-1001.
34. B. Sakmann and E. Neher, *Annu Rev Physiol*, 1984, **46**, 455-472.
35. C. H. Lee, D. Poburko, K. H. Kuo, C. Y. Seow and C. van Breemen, *Am J Physiol Heart Circ Physiol*, 2002, **282**, H1571-1583.
36. S. Sandhiya and S. A. Dkhar, *Indian J Med Res*, 2009, **129**, 223-232.

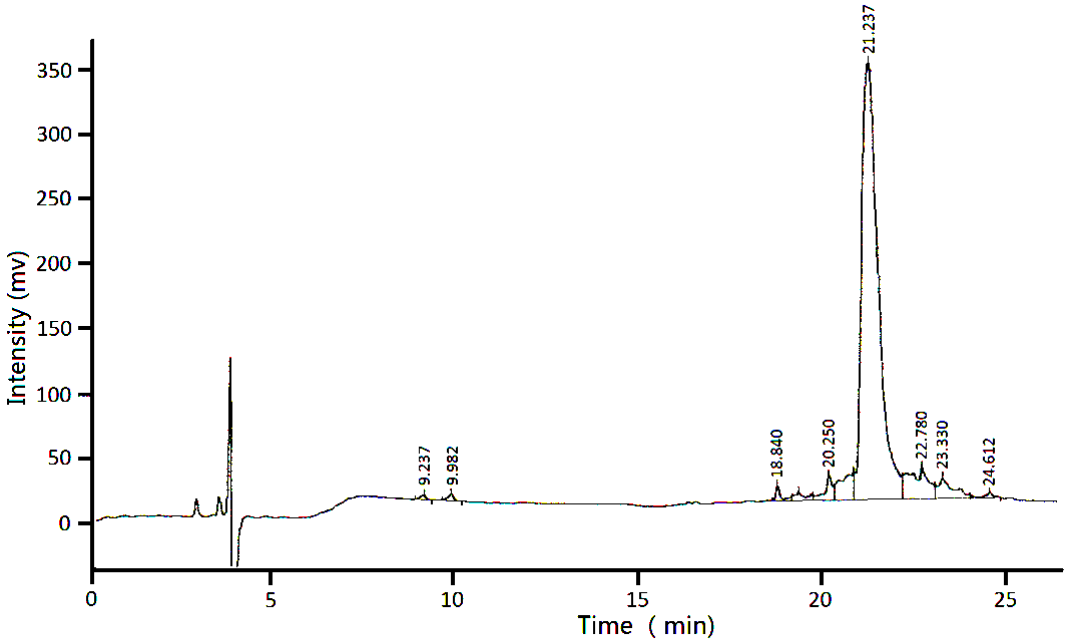

Fig. 1. Purification of the synthetic TRP-PK1 was confirmed by RP-HPLC. The synthetic peptide was applied to a C18 column (10 mm × 250 mm) pre-equilibrated with 0.1% TFA. Elution was performed with a linear gradient of 55%–85% acetonitrile at a flow rate 3.0 mL/min.

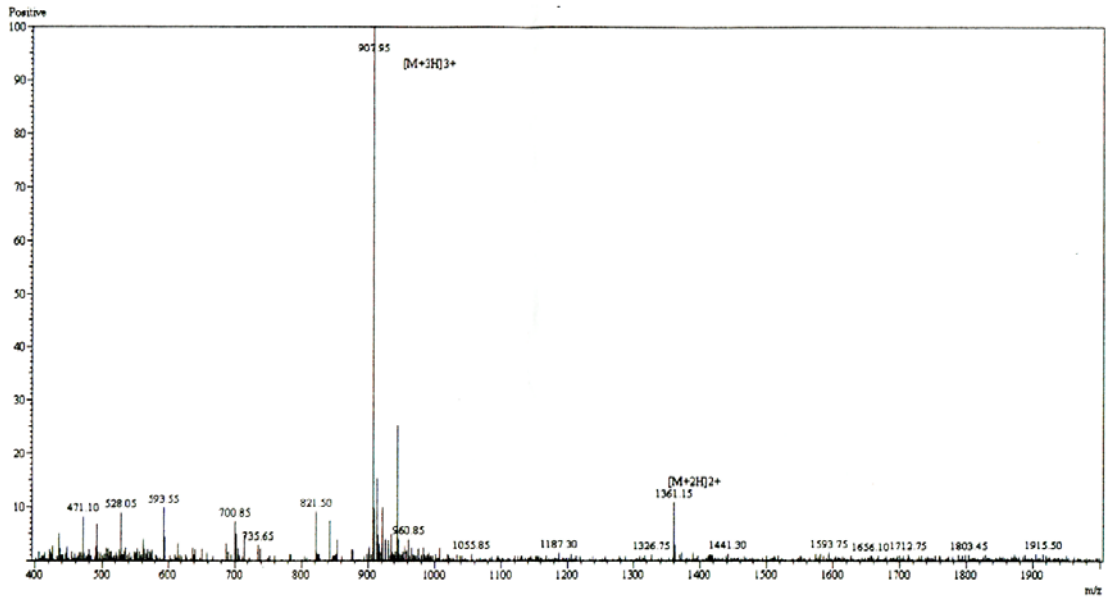

Fig. 2. The synthetic peptide purified by RP-HPLC was confirmed by ESI mass spectrometer.

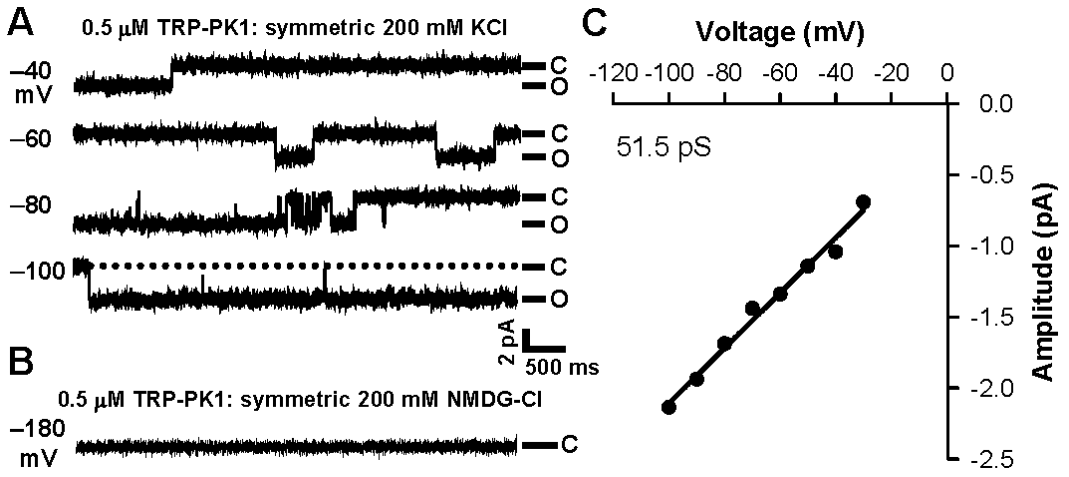

Fig. 3. Single-channel current of TRP-PK1 channel in liposomes. (A) Cell-attached single channel currents of TRP-PK1 from −40 mV to −100 mV recorded in POPC liposomes with symmetric 0.2 M KCl in the presence of 0.5 μM TRP-PK1. (B) Cell-attached single channel recording at −180 mV in POPC liposomes with symmetric 0.2 M NMDG-Cl in the presence of 0.5 μM TRP-PK1. (C) Current-voltage relationship of TRP-PK1. The estimated conductance of the channel is 51.5 pS.

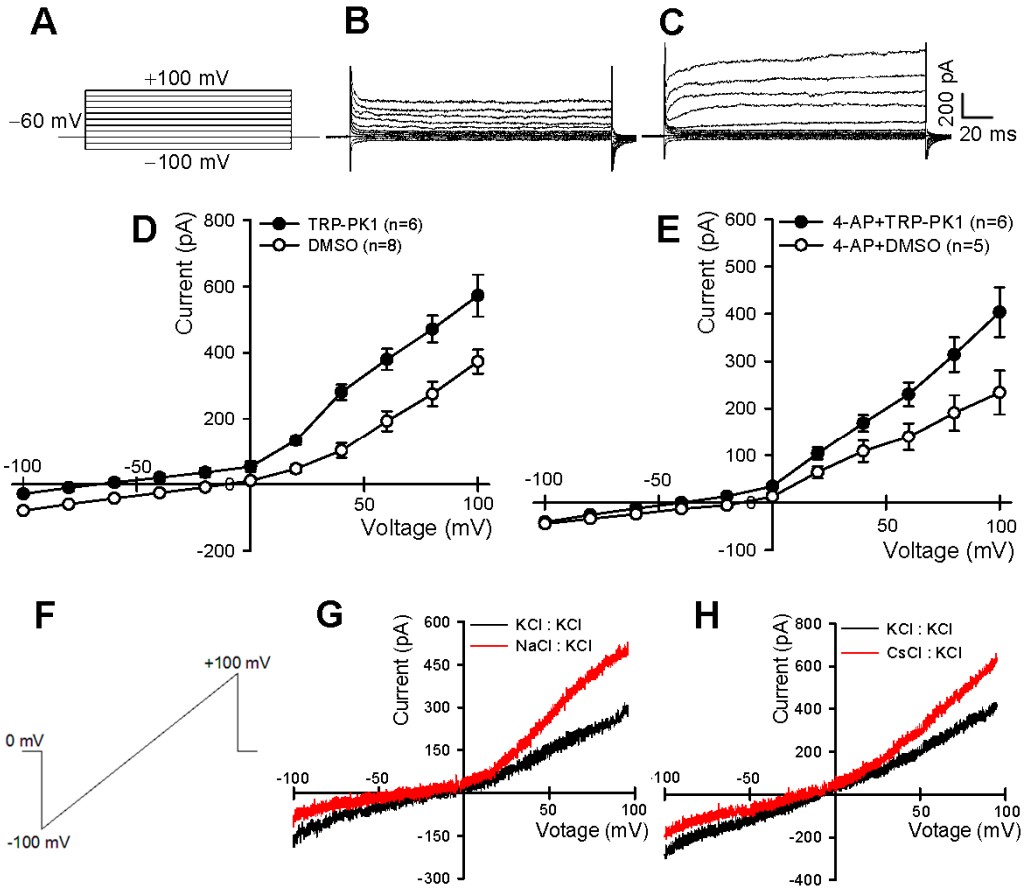

Fig. 4. Whole-cell current and cation ion permeability of TRP-PK1 channel in HEK293 cells. (A-C) Representative traces showing stimulation protocol of whole-cell recording (A), K^+ current before (B) and after (C) 5 μM TRP-PK1 application. (D-E) Current–voltage relationships obtained in the absence (○) and presence (●) of 5 μM TRP-PK1 in HEK 293 cells without (D) or with (E) 100 μM 4-AP treatment. All data are means ± SE. n=5-8. (F-H) Traces showing the stimulation protocol of ramp recording (F), the changes in reverse potential and whole cell current when extracellular solutions were changed from 150 mM KCl (black traces) to 150 mM NaCl (G) or CsCl (H) (red traces), respectively. 5 μM TRP-PK1 always existed in the extracellular solutions.

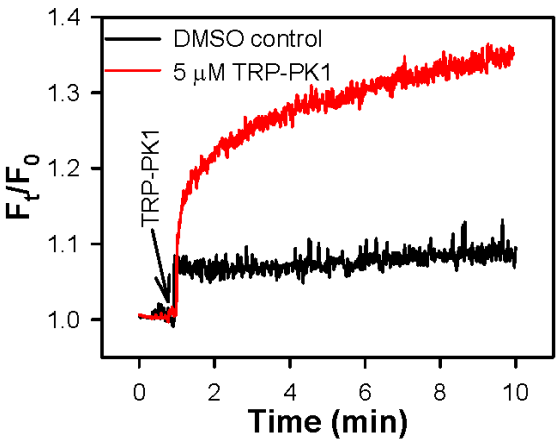

Fig. 5. The function of TRP-PK1 to mediate K^+ ions. Traces showing that the application of 5 μM TRP-PK1 significantly enhanced the PBFI fluorescence signal. Inside vesicles: 100 mM NMDG-Cl, 500 μM PBFI, pH 6.8. Outside vesicles: 100 mM KCl, pH 6.8. TRP-PK1 (5 μM final concentration) was added at the time indicated at the arrow. Changes in the intravesicular K^+ concentration were displayed as the ratio of fluorescence relative to the intensity before the application of extracellular TRP-PK1 (Ft/F0).

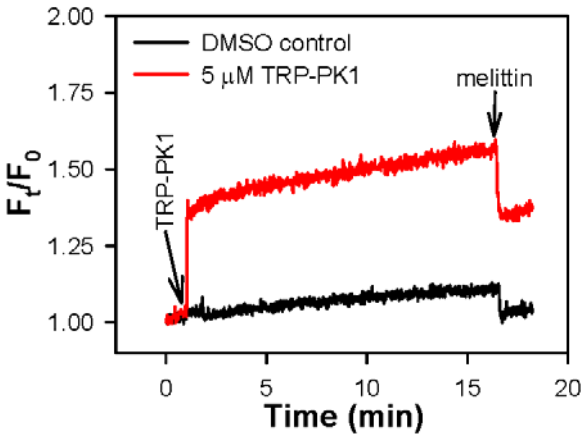

Fig. 6. The effect of TRP-PK1 on regulating liposome membrane potential. Traces showing that the application of 5 μM TRP-PK1 hyperpolarized the membrane potential of liposomes. Inside vesicles: 100 mM KCl, pH 6.8. Outside vesicles: 100 mM NaCl, 60 nM safranin O, pH 6.8. TRP-PK1 (5 μM final concentration) was added at the time indicated at the arrow. At the end of the experiments, 10 μM melittin was added to lyse the lipid membrane of liposomes. Changes in liposome membrane potential were displayed as the ratio of fluorescence relative to the intensity before the application of extracellular TRP-PK1 (Ft/F0).

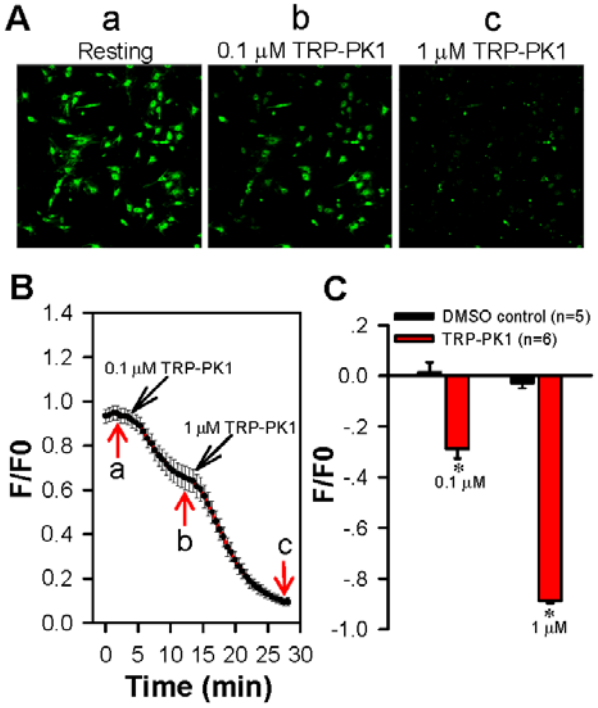

Fig. 7. The effect of TRP-PK1 on the membrane potential regulation in vascular smooth muscle cells. (A) Images showing the membrane potential change of the primary cultured vascular smooth muscle cell of mouse. The applications of 0.1 and 1 μM TRP-PK1 markedly decreased the fluorescence signal. The membrane potential was probed by 100 nM $DiBAC_4(3)$ dye and three images (a, b, c) were from different stages in the trace of (B). (B, C) Trace and summary of data showing the membrane potential change of the primary cultured mouse vascular smooth muscle cells. The applications of 0.1 and 1 μM TRP-PK1 (C, at the arrows) markedly hyperpolarized the resting membrane potential of the primary cultured mouse vascular smooth muscle cell. Mean ± SE. **P* < 0.05 compared with DMSO control. n=5-6 independent experiments.

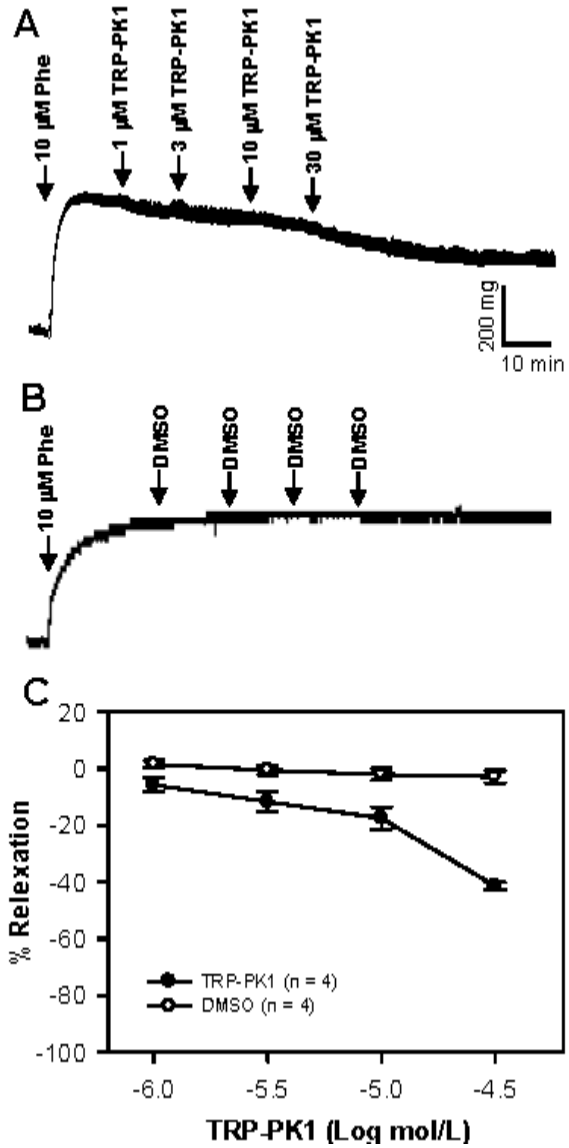

Fig. 8. Vasorelaxant effect of TRP-PK1 on mouse aorta. (A, B) The original traces showing that 1 μM to 30 μM TRP-PK1 (A) and DMSO control (B) induced vessel relaxation in 10 μM phenylephrine (Phe)-preconstricted mouse aortic rings. (C) Concentration-dependent curves for the vasorelaxant effects of TRP-PK1 and solvent control (DMSO) on the mouse aortic rings preconstricted by 10 μM Phe. Each point represents the mean ± SE. (n=4).

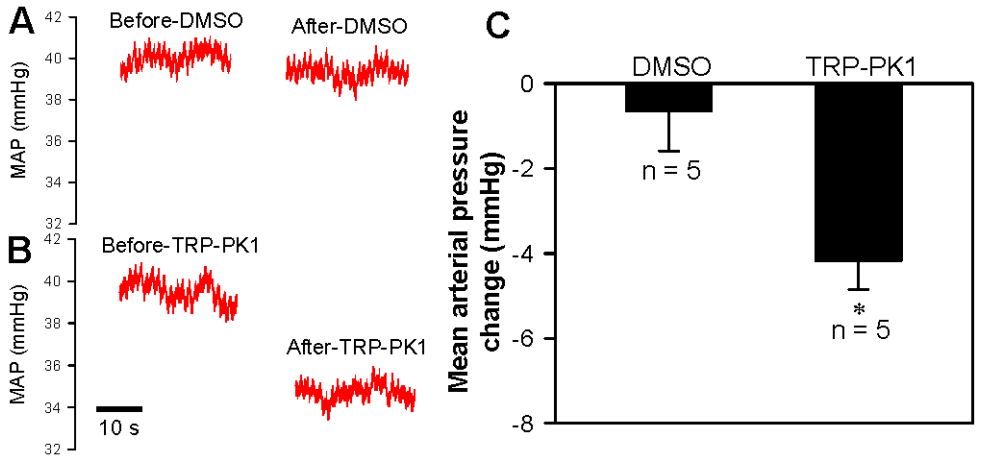

Fig. 9. Effect of TRP-PK1 on the mouse mean arterial pressure. Original traces represent the mouse mean arterial pressure before and after DMSO control (A) and TRP-PK1 (B) (1 mg/25 g, w/w) injection for 10 min. (C) Summary of data showing changes in the mouse mean arterial pressure in response to DMSO and TRP-PK1 injection. Mean ± SE. **P* < 0.05 compared with DMSO control. n=5.

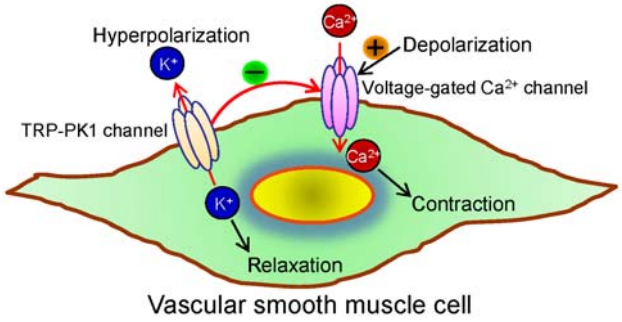

Fig. 10. Schematic showing the mechanism of the TRP-PK1 channel to regulate the vascular smooth muscle cell (VSMC) membrane potential, voltage-gated Ca^{2+} channel opening and VSMC contraction.